

# Tracing the development of dust around evolved stars: The case of 47 Tuc

Th. Lebzelter, Th. Posch

*Institut für Astronomie, Türkenschanzstraße 17, A-1180 Wien, Austria*

lebzelter@astro.univie.ac.at

K. Hinkle

*NOAO, P.O.Box 26732, Tucson, AZ 85726, USA*

P.R. Wood

*RSAA, Mount Stromlo Observatory, Weston, ACT 2611, Australia*

J. Bouwman

*Max-Planck-Institut für Astronomie (MPIA), Königstuhl 17, D-69117 Heidelberg, Germany*

## ABSTRACT

We observed mid-infrared ( $7.5\text{--}22\,\mu\text{m}$ ) spectra of AGB stars in the globular cluster 47 Tuc with the *Spitzer* telescope and find significant dust features of various types. Comparison of the characteristics of the dust spectra with the location of the stars in a  $\log P$ - $K$ -diagram shows that dust mineralogy and position on the AGB are related. A  $13\,\mu\text{m}$  feature is seen in spectra of low luminosity AGB stars. More luminous AGB stars show a broad feature at  $11.5\,\mu\text{m}$ . The spectra of the most luminous stars are dominated by the amorphous silicate bending vibration centered at  $9.7\,\mu\text{m}$ . For 47 Tuc AGB stars, we conclude that early on the AGB dust consisting primarily of Mg-, Al- and Fe oxides is formed. With further AGB evolution amorphous silicates become the dominant species.

*Subject headings:* dust — Spitzer — stars: AGB and post-AGB — stars: mass loss

## 1. Introduction

Stars on the Asymptotic Giant Branch (AGB) represent the final evolutionary stage of low- to intermediate mass stars. The large AGB mass-loss rates play a key role in the

cosmic circuit of matter. This mass loss consists of both gas and (sub-)micron-sized solid “dust” particles. Dust in the circumstellar shells of AGB stars leads to a significant change in the overall spectral energy distribution compared to dust-free objects. It attenuates stellar radiation in the blue and visual range and re-radiates corresponding emission at mid-infrared wavelengths (‘infrared excess’). The spectrum of the infrared excess contains broad spectral features characteristic of specific dust species.

Up to now, dust properties of AGB stars could be determined only for samples in the galactic disk and bulge (e.g. Omont et al. 2003). The IRAS and ISO missions created large databases of mid- and far-IR spectra of dust-producing stars. Analysis of these spectra led to basic insights e.g. into the relation between dust properties and stellar C vs. O abundances or total mass loss rates (e.g. Molster & Waters 2003). However, as the disk and bulge samples are inhomogeneous with respect to individual metallicities and masses – which both influence the production of dust – several questions remained open. One main open issue concerns the interrelation between the dust composition, stellar variability, and evolutionary status of an AGB star. In contrast to stellar samples in the galactic disk and bulge, globular clusters (GCs) make possible observation of stellar samples with well-defined, homogeneous parameters.

## 2. Sample selection and data reduction

Among the GCs, 47 Tuc (NGC 104,  $[\text{Fe}/\text{H}] = -0.76$ , Briley et al. 1995) is especially suited for a study correlating AGB stellar parameters and dust spectral signatures. This cluster has a well populated AGB with indications of dust formation due to considerable IR excesses (van Loon et al. 2006, Ramdani & Jorissen 2001). Lebzelter et al. (2005) and Lebzelter & Wood (2005) were able to assign fundamental or overtone pulsation modes to most of the 47 Tuc AGB variables. Overtone pulsators exclusively populate the lower part of the AGB, while fundamental mode pulsators are only found at high luminosities. The NIR velocity amplitude was found to strongly increase during the transition from overtone to fundamental mode and to further increase along the fundamental mode sequence with luminosity. Based on these findings, we selected 10 targets distributed over the AGB pulsation modes and luminosity range for observation with Spitzer. One star, V13<sup>1</sup>, shows a short primary and a long secondary period (Lebzelter et al. 2005). To this sample we added V18, a star located between the fundamental and the overtone mode pulsators with a strong infrared excess (Ramdani & Jorissen 2001). It was suggested by Lebzelter et al. (2005) that

---

<sup>1</sup>Throughout this paper, variables are named according to Clement et al (2001).

this star is currently in the luminosity minimum following a thermal pulse. The upper left panel of Fig. 1 gives an overview on the location of the various variables in the logP- $K$  diagram.

For these 11 targets low resolution *Spitzer* spectra have been obtained between  $7.6 - 21.7 \mu\text{m}$  during Cycle 1. Our spectra are based on the **droopres** products processed through the S13.2.0 version of the *Spitzer* data pipeline. Partially based on the **SMART** software package (Higdon et al. 2004), these intermediate data products were further processed using spectral extraction tools developed for the "Formation and Evolution of Planetary Systems" (FEPS) *Spitzer* science legacy team. The spectra were extracted using a 6.0 pixel and 5.0 pixel fixed-width aperture in the spatial dimension for the observations with the first order of the short- ( $7.6 - 14 \mu\text{m}$ ) and the second and third order of the long-wavelength ( $14 - 21.7 \mu\text{m}$ ) modules, respectively. The background was subtracted using associated pairs of imaged spectra from the two noddled positions along the slit, also eliminating stray light contamination and anomalous dark currents. Pixels flagged by the data pipeline as being "bad" were replaced with a value interpolated from an 8 pixel perimeter surrounding the errant pixel. The low-level fringing in the low-resolution spectra at wavelengths longer than  $20 \mu\text{m}$  was removed using the **irsfinge** package (Lahuis & Boogert 2003). The spectra are calibrated using a spectral response function derived from IRS spectra and Cohen stellar models for a suite of calibrators provided by the *Spitzer* Science Centre. To remove any effect of pointing offsets, we matched orders based on the wavelength dependend point spread function of the IRS instrument, correcting for possible flux losses. The relative errors between spectral points within one order are dominated by the noise on each individual point and not by the calibration. We estimate a relative flux calibration across an order of  $\approx 2 \%$  and an absolute calibration error between orders/modules of  $\approx 5 \%$ .

The mid-IR (MIR) SED consists of a photospheric continuum component and various dust features on top of it. To obtain a clear view on the signatures of the dust we subtracted a blackbody curve representing the photosphere. For this purpose we obtained parallel near infrared photometry (JHKL) at Siding Spring Observatory (SSO). The blackbody temperatures (3400-3900 K) were derived from  $J - K$  values using the relation by Houdashelt et al. (2000). The flux levels of the blackbodies were chosen such as to fit the near infrared flux levels. For sample stars with low mass loss rates we assume that the infrared excess will not significantly affect  $J - K$ . Fig. 2 gives an example of a spectrum before and after blackbody subtraction. In the following we will present and discuss only continuum subtracted spectra. The chosen continuum subtraction method naturally introduces some uncertainty in the derived residual dust emission, but this uncertainty does not affect the positions and relative strengths of the various dust features on which this paper is focused.

### 3. The MIR spectra of AGB stars in 47 Tuc

#### 3.1. Phenomenology of the dust spectra

V5, V6 and V7 can be fitted nicely with single blackbodies of about 3700 to 3900 K and must be nearly dust-free. Dust features were detected in the remaining 8 of the 11 sample stars. The three dominant dust features are located at approximately 9.7, 11.5 and 13  $\mu\text{m}$ . Additionally, broad features at 18–20  $\mu\text{m}$  are visible. However, not all features are visible in all stars. In Fig. 1, we show the dust spectra and the location of the corresponding stars in the logP- $K$  diagram. V13 is presented separately in Fig. 2. From the logP- $K$  values we can form three groups among the sample stars. The spectra of pairs V5/V6, V4/V8 and V1/V2 are very similar, suggesting a typical spectrum is associated with a specific location in the logP- $K$ -diagram. An interesting case is V3 with similar logP- $K$  values as V1/V2. The V3 spectrum has a very weak dust feature sitting on top of a broad mid-IR emission with a wavelength dependent slope. This slope can be roughly approximated by a blackbody curve on top of which a weak 9.7  $\mu\text{m}$  feature stands out. While not obvious, this is the same spectral signature as in V1/V2. In 3.3 we further discuss these differences as a function of stellar variability.

The change of the dust features along the AGB is in agreement with earlier studies on the relation between dust properties and stellar parameters. While previous works on this subject (e.g. Onaka et al. 1989, Sloan & Price 1996, Hron et al. 1997, Heras & Hony 2005) refer to an inhomogeneous samples of stars, our GC spectra minimize possible effects of such inhomogeneities. At the lower luminosity end of the AGB, hardly any dust is present. Effective dust production seems to start only after the star reaches the luminosity of V21 corresponding to a value of approximately 2000  $L_{\odot}$  (cf. Lebzelter & Wood 2005). The 13  $\mu\text{m}$  feature clearly dominates the spectrum at this luminosity. Changing from V21 to V4 brings about a switch in pulsation mode from overtone to fundamental mode and a strong increase in the observed velocity amplitude. The related change in the MIR spectrum is an increase in the 11.5  $\mu\text{m}$  feature, a decrease in the strength of the 13  $\mu\text{m}$ , and the occurrence of a 9.7  $\mu\text{m}$  feature. Going to even higher luminosities leads to V1 with its dominating 9.7  $\mu\text{m}$  feature and only a very weak indication for the 11.5  $\mu\text{m}$  feature, sitting on the long wavelength side of the 9.7  $\mu\text{m}$  emission.

Summarizing these observations, we can say that the 13  $\mu\text{m}$  feature appears in the least evolved stars, later loses importance relative to the 11.5  $\mu\text{m}$  peak and a feature at 9.7  $\mu\text{m}$  and finally vanishes completely in the highest luminosity stars. The latter are dominated completely by the 9.7  $\mu\text{m}$  emission.

### 3.2. Identification of the dust features

Among the observed emission bands only the  $9.7\,\mu\text{m}$  feature has a generally accepted identification, amorphous Mg-Fe-silicate (see, e.g., Dorschner et al. 1995 for optical constants). No consensus exists on the carriers for the broad  $11.5\,\mu\text{m}$  band, the narrow  $13\,\mu\text{m}$  band, and the various features between 17 and  $20\,\mu\text{m}$ . Since the sample stars are all spectral type K or M the dust species must be oxides.

First detected in IRAS spectra (Little-Marenin & Little 1988), the  $13\,\mu\text{m}$  band was identified as part of a ‘three-component-feature’ consisting of a  $9.7$ ,  $\sim 11$ , and the  $13\,\mu\text{m}$  band itself. Our spectra of 47 Tuc V4 and V8 show the ‘three-component-feature’. The  $13\,\mu\text{m}$  feature is likely an Al-O stretching vibration. The carrier has been identified as either corundum ( $\alpha\text{-Al}_2\text{O}_3$ , Glaccum 1995, DePew, Speck & Dijkstra 2006) or spinel ( $\text{MgAl}_2\text{O}_4$ , Posch et al. 1999, Fabian et al. 2001, Heras & Hony 2005).

The origin of the broad  $11.5\,\mu\text{m}$  band in spectra of O-rich AGB stars has been extensively discussed (e.g. Stencel et al. 1990, Lorenz-Martins & Pompeia 2000, Egan & Sloan 2001, Posch et al. 2002, Heras & Hony 2005). Although it is especially difficult to identify uniquely such a broad solid state band, there remains little doubt that amorphous  $\text{Al}_2\text{O}_3$  is the band carrier in this case.<sup>2</sup>

The band (or double-band) at  $18\text{--}20\,\mu\text{m}$  is most distinctly seen in V1 ( $18\,\mu\text{m}$ ), V4 ( $18+20\,\mu\text{m}$ ), V8 ( $20\,\mu\text{m}$ ), V13 ( $20\,\mu\text{m}$ ), V18 ( $18+20\,\mu\text{m}$ ) and V21 ( $20\,\mu\text{m}$ ). The observed differences in the positions of the feature’s maxima probably indicate a transition from a crystalline oxide (with a composition between MgO to FeO, see Posch et al. 2002) as the dominant opacity source in the  $19\text{--}21\,\mu\text{m}$  region to an amorphous silicate’s bending vibration as the primary emission mechanism. Sloan et al. (2003) found a correlation between the strengths of the  $13$  and  $20\,\mu\text{m}$  features.

In Fig. 2 we show the spectrum of V13 with the band identifications for the oxide dust features suggested above. The spectrum of V13 is further discussed in section 3.4.

### 3.3. Variability of the mid-IR spectra

At least for fundamental-mode AGB pulsators cyclic variability leads to significant changes in size and  $T_{\text{eff}}$  of the star. These could effect the observed MIR spectra through

---

<sup>2</sup> Amorphous  $\text{Al}_2\text{O}_3$  is sometimes called ‘corundum’ in the literature. However, this name should be reserved for the crystalline  $\alpha$ -phase of  $\text{Al}_2\text{O}_3$ .

cyclic changes in both dust production and photospheric flux. From Spitzer we have only one observational epoch for each star. However, additional information provides indications of the impact on the mid-infrared spectrum.

Our sample contains the three miras, V1, V2, and V3, all sharing a similar location in the logP-K-diagram. Their spectra show the same dust features, but with a very different contrast against the photospheric background. From the simultaneous  $K$  photometry, we estimate that V1 was observed close to light maximum, while V2 and V3 were close to minima. We speculate that the background is related to the pulsation phase. This is seen in model atmospheres (Aringer 2005). Phase dependent background can possibly explain the difference between our spectrum of V8 and one published by van Loon et al. (2006). While dust features are quite obvious in the Spitzer observation, the van Loon spectrum taken from the ground shows no features at all. The  $K$  amplitude of V8 is too small to safely estimate the phase from the observed  $K$  magnitude.

### 3.4. Two peculiar cases: V13 and V18

Two stars do not seem to fit in the dust evolution scenario described in 3.1: V13 and V18 which both have IR excess emission much too strong in relation to their position in the logP-K diagram. The residual dust emission spectrum of V13 (Fig. 2) is almost devoid of a  $10\mu\text{m}$  band. This alone is not surprising, because it also is the case for V21. However, V13 is almost 1 mag fainter in  $K$  than V21. The spectra of both V13 and V21 are characterized by pronounced 11.5, 13 and  $20\mu\text{m}$  peaks. V18 shows a spectrum very similar to the mira V1, i.e. it is dominated by a  $9.7\mu\text{m}$  silicate dust feature, yet is  $\sim 1.25$  magnitude fainter at  $K$ .

What properties of V13 enable the formation of dust? The only remarkable pulsational characteristic of V13 is its long secondary period. This long period is also clearly visible in the radial velocity (Lebzelter et al. 2005) as well as photometric variation. The length of the secondary period has not been determined accurately but seems to fall onto the Wood et al. (1999) P-L sequence "D". The interpretation of this sequence in terms of stellar pulsation or binarity is still not clear (e.g. Wood 2006).

We interpret the dust spectrum of V18 in the light of the earlier suggestion that this star is currently undergoing a thermal pulse event. V18 would then have an interpulse luminosity and dust spectrum similar to that of an 47 Tuc mira, e.g. V1. According to evolution models of thermally pulsing AGB stars by Vassiliadis & Wood (1993), a significant disturbance of the typical pulsation period of a star occurs during the thermal pulse (cf. their Fig. 3), which

would explain the strange location of V18 in the logP- $K$  diagram.

#### 4. Consequences for the evolution of dust on the AGB

Our evolutionary sequence of the dust spectra indicates that oxygen-rich AGB stars first form dust rich in oxides of aluminum and magnesium (specifically,  $\text{Al}_2\text{O}_3$ -,  $\text{MgAl}_2\text{O}_4$ - and  $(\text{Mg,Fe})\text{O}$ -). As a star climbs up the AGB, the original aluminum-magnesium oxide dust contributes less to the emergent dust shell spectra, while the relative strength of amorphous silicate bands, especially the one at  $9.7\,\mu\text{m}$ , increases. This scenario is in agreement with considerations published by Stencel et al. (1990) linking this evolutionary sequence to the higher electron affinity of Al (compared to Si) to oxygen. It is the high binding energy of solid Al oxides which enables them to condense at much higher temperatures than silicates (see, e.g., Gail 2003, Fig. 4). Once the Al oxides have formed, silicates will start to precipitate on their surfaces which gradually leads to a transition to a silicate dominated dust spectrum. Hron et al. (1997) pointed out that the  $13\,\mu\text{m}$  feature reaches significant strength only in a narrow range of effective temperatures and optical depths. They proposed an evolutionary sequence in the course of which the carrier of this band would be gradually incorporated into amorphous silicates with increasing mass-loss rate. Most recent model calculations by Voitke (A&A submitted) indicate that  $\text{Al}_2\text{O}_3$  can exist closer to the star while silicates are formed at larger distances, i.e. once effective mass loss has set in.

A similar scenario for aluminum-magnesium oxide/silicate dust evolution has been proposed by Onaka et al. (1989). They derive a relation between the asymmetry factor of the light curve and the importance of the various dust features with the stars exhibiting the strongest asymmetries showing the most pronounced silicate emission. The asymmetry of the light curve can be related to the strengths of the shock front occurring during the cyclic pulsation as discussed by Onaka and coworkers. Lebzelter et al. (2005) showed that the near-IR velocity amplitude increases along the AGB of 47 Tuc. Thus a relation between pulsational properties and the dust composition can be expected. The necessity of taking into account pulsation characteristics as an additional factor beside luminosity is illustrated by comparing the spectra of V21 and V4 (Fig. 1). The overall shape of the mid-infrared spectrum – but not the dust features that occur – seems additionally to depend on the pulsational phase. A more complete discussion of the individual dust spectra will be given in a forthcoming paper, where we will give a more detailed presentation of the spectra and a comparison with combined atmospheric and dust models.

This work is based on observations made with the Spitzer Space Telescope, which is operated

by the Jet Propulsion Laboratory, California Institute of Technology under a contract with NASA. Support for this work was provided by NASA through an award issued by JPL/Caltech. TL acknowledges funding through FWF project P18171. PRW received partial funding support from an Australian Research Council Discovery Grant. JB acknowledges support from the EU Human Potential Network contract No. HPRN-CT-2002000308. We thank H.-P. Gail and J. Hron for fruitful discussions on this paper.

## REFERENCES

- Aringer B. 2005, in: Käufel H. U., et al. (eds.), *High Resolution Infrared Spectroscopy in Astronomy*, Springer, p. 303
- Briley, M. M., Smith, V. V., King, J. R., & Lambert, D. L., 1995, *Nature*, 383, 604
- Clement C. M., et al. 2001, *AJ*, 122, 2587
- DePew K., Speck A., & Dijkstra C., 2006, *ApJ*, 640, 971
- Dorschner J., Begemann B., Henning Th., Jaeger C., & Mutschke H. 1995, *A&A*, 300, 503
- Egan M.P., & Sloan G.C., 2001, *ApJ*, 558, 165
- Eriksson T. S., Hjortsberg A., Niklasson G. A., & Granqvist C. G. 1981, *Appl. Optics*, 20, 2742
- Fabian D., Posch Th., Mutschke H., Kerschbaum F., & Dorschner J., 2001, *A&A*, 373, 1125
- Gail H.-P., 2003, in: Th. Henning (ed.), *Astromineralogy*, *Lecture Notes in Physics*, no. 609, p. 55
- Glaccum W., 1995, in: M.R. Haas et al. (eds.), *ASP Conf. Ser.* 73, p. 395
- Henning Th., Begemann B., Mutschke H., & Dorschner J. 1995, *A&AS*, 112, 143
- Heras A.M., Hony S., 2005, *A&A*, 439, 171
- Higdon S.J.U., et al. 2004, *PASP*, 116, 975
- Houdashelt M. L., Bell R. A., & Sweigart A. V., 2000, *AJ*, 119, 1448
- Hron J., Aringer B., Kerschbaum F., 1997, *A&A*, 322, 280



- Lahuis, F., & Boogert, A. 2003 , in *SFChem 2002: Chemistry as a Diagnostic of Star Formation*, Edited by Charles L. Curry & Michel Fich, NRC Press, Ottawa, Canada, 335.
- Lebzelter T., Wood P.R., Hinkle K.H., Joyce R.R., Fekel F.C., 2005, *A&A*, 432, 207
- Lebzelter T., Wood P.R., 2005, *A&A*, 441, 1117
- Little-Marenin I. R., & Little S. J. 1988, *ApJ*, 333, 305
- Lorenz-Martins S., & Pompeia L., 2000, *MNRAS*, 315, 856
- Molster F. J., Waters L.B.F.M., 2003, in: Th. Henning (ed.), *Astromineralogy, Lecture Notes in Physics*, no. 609, p. 121
- Omout A. et al., 2003, *A&A*, 403, 975
- Onaka T., de Jong T. & Willems F. J., 1989, *A&A*, 218, 169
- Ossenkopf V., Henning Th., & Mathis J. S. 1992, *A&A*, 261, 567
- Posch Th., Kerschbaum F., Mutschke H., et al., 1999, *A&A*, 352, 609
- Posch Th., Kerschbaum F., Mutschke H., Dorschner J., Jäger C., 2002, *A&A*, 393, L7
- Ramdani A., Jorissen A., 2001, *A&A*, 372, 85
- Sloan G.C., & Price S.D., 1998, *ApJS*, 119, 141
- Sloan, G.C., Kraemer, K.E., Goebel, J.H., Price, S.D., 2003, *ApJ*, 594, 483
- Stencel R.E., Nuth J.A., Little-Marenin I.R., Little S.J., 1990, *ApJ*, 350, L45
- van Loon J.Th., McDonald I., Oliveira J.M., et al., 2006, *A&A*, 450, 339
- Vassiliadis E., & Wood P. R. 1993, *ApJ*, 413, 641
- Wood P. R., et al. 1999, *IAU Symp. 191: Asymptotic Giant Branch Stars*, 191, 151
- Wood P. R. 2006, *Memorie della Società Astronomica Italiana*, 77, 76

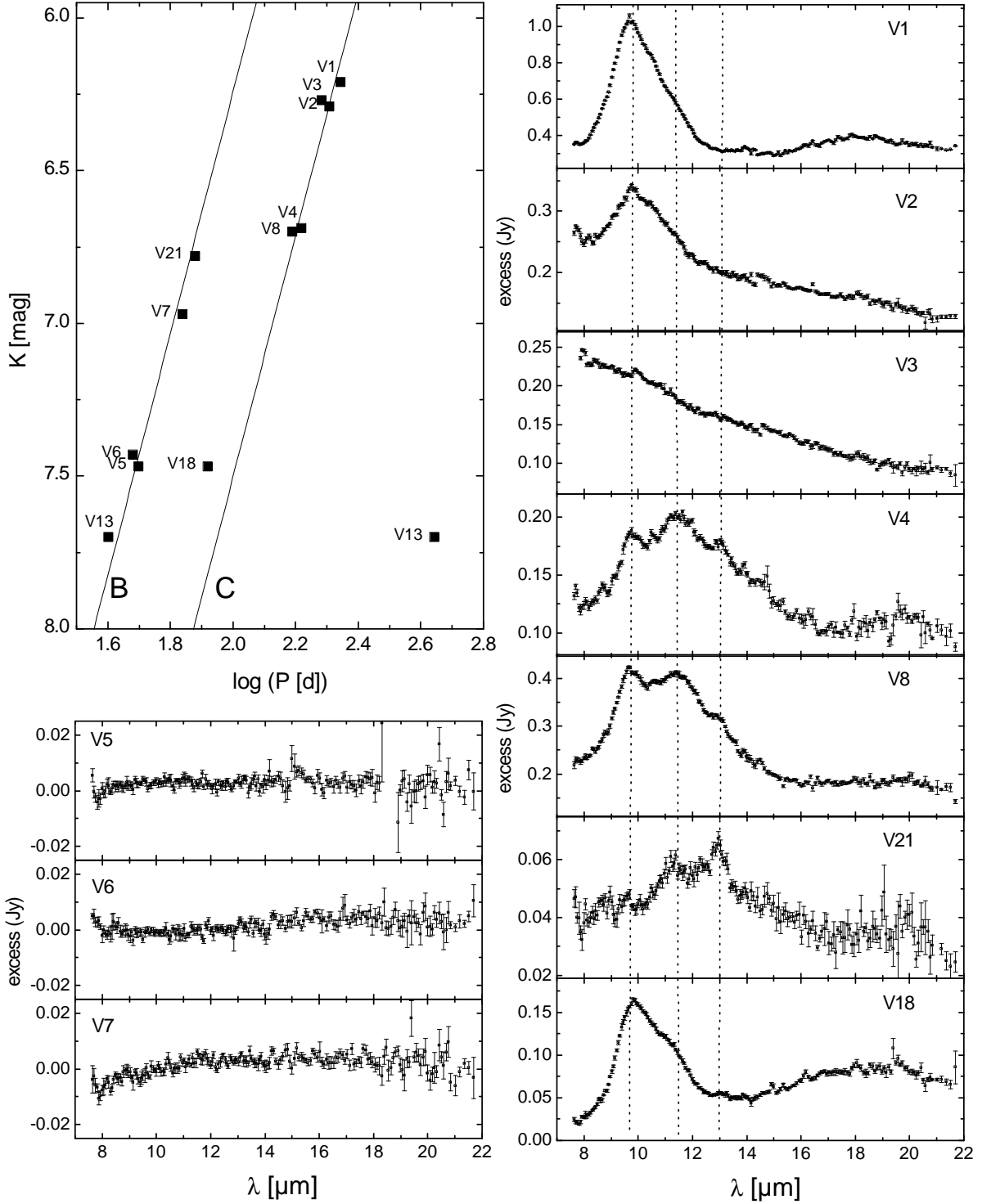


Fig. 1.— Development of dust spectra in 47 Tuc. *Right and lower left:* Spitzer spectra of the AGB stars in 47 Tuc (for V13 see Fig. 2) with blackbody curves subtracted (see text). Spectra are plotted as individual data points with errors bars derived from the difference between the two nod positions. The features at 9.7, 11.5 and 13  $\mu$ m are indicated by vertical dashed lines. *Top left corner:* logP-K-diagram of the sample stars adapted from Lebzelter et al. (2005). Solid lines mark the locations of overtone (B) and fundamental mode (C) radial pulsators (Wood et al. 1999). V13 is plotted with both of its periods.

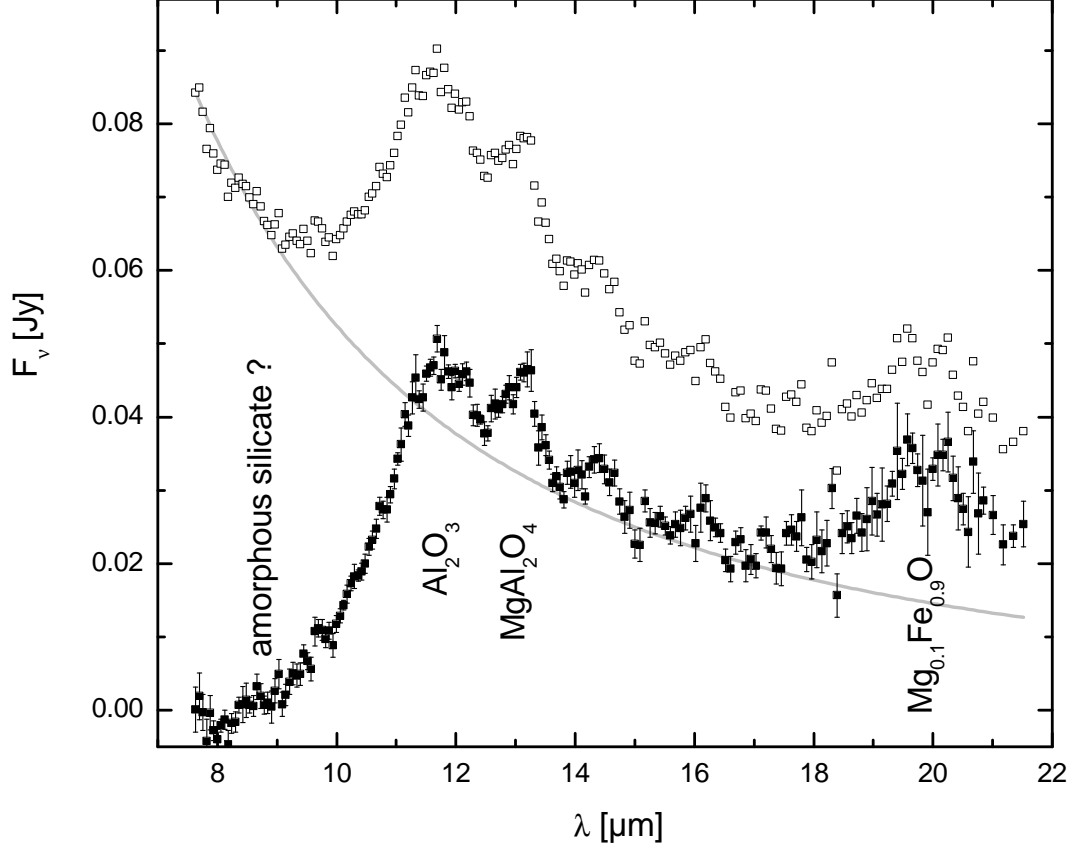


Fig. 2.— The Spitzer mid-IR spectrum of V13 (open symbols) and the residual dust emission (filled symbols). The grey line gives the blackbody used for continuum subtraction. Error bars are derived from the difference of the two nod positions. The indicated dust feature peak positions are from the optical constants published for amorphous  $\text{Al}_2\text{O}_3$  (Eriksson et al. 1981), crystalline  $\text{MgAl}_2\text{O}_4$  (Fabian et al. 2001),  $\text{Mg}_{0.1}\text{Fe}_{0.9}\text{O}$  (Henning et al. 1995), and (hardly detectable) amorphous silicate (Ossenkopf et al. 1992).